PHOTOPRODUCTION AT HERA*

SAMPA BHADRA

York University, Department of Physics
4700 Keele Street, Toronto, Canada
and
Deutsches Elektronen Synchrotron
Notkestrasse 85, 22603 Hamburg, Germany

(Received November 10, 1994)

Results from photoproduction at HERA are presented, including cross section measurements for ρ^0, ϕ, and J/ψ production. We have found jets which are a signature for hard scattering processes. An analysis of two-jet events allows us to probe the structure of both the photon and the proton. Comparisons are made of di-jet production to predictions from LO QCD, using different structure functions of the proton and photon. We have searched for hard scattering in diffractive events and compared our results to models where the exchanged pomeron is composed of partons.

PACS numbers: 13.60. -r

1. Introduction

The gauge interactions of the electron and photon are well known, but the interaction of the photon with hadrons or photons is less well understood. HERA is an electron– (26.7 GeV) proton (820 GeV) collider. However, the large flux of quasi-real photons ($Q^2 \approx 0$) from the electrons makes it an ideal machine to explore the nature and structure of the photon. The average centre of mass energy $W_{\gamma p} \approx 200$ GeV is a factor of ten higher than in previous experiments. Hence it is interesting to compare our results to theoretical models which are sensitive to the high energy behaviour, since pre-HERA predictions vary widely.

An excellent review by Storrow [1] brings some order to the varied and sometimes confusing classification of photon interactions. The classification is made in terms of the P_t scale, where "low P_t" is the region where the

* Presented at the XXXIV Cracow School of Theoretical Physics, Zakopane, Poland, June 1–10, 1994.

differential cross section is well described by an exponential behaviour in P_t. This soft physics is non-perturbative and not presently calculable in QCD. The subprocesses contributing are elastic, inelastic diffractive, and non-diffractive. The slope in P_t at larger values is more like a power law, and in this region of hard scattering, we can use perturbative QCD to describe the scattering process. The photon interacts directly, or resolves itself before interacting. One important distinction between photons and hadrons is that photons can interact directly with the partons of the proton, while hadrons only interact through their constituent partons.

The fractional momentum x_γ (x_p) carried by the parton in the photon (proton) can be written as

$$x_\gamma = \frac{E_t^1 e^{-\eta_1} + E_t^2 e^{-\eta_2}}{2E_\gamma}, \quad x_p = \frac{E_t^1 e^{\eta_1} + E_t^2 e^{\eta_2}}{2E_p}, \tag{1}$$

where E_γ (E_p) is the photon (proton) energy, E_t^1, E_t^2 refer to the transverse energies, and η_1, η_2 to the pseudorapidities of the outgoing partons. The direct component, where all the energy of the photon enters the reaction, has $x_\gamma = 1$, while the resolved component will result in a value less than 1. We use the variables x_γ and x_p to probe the quark and gluon content of the photon and proton.

2. Cross section measurements of $\rho^0, \phi, J/\psi$

Photoproduction results from the 1992 and 1993 data taking period of HERA have been obtained from about 25 nb^{-1} and 500 nb^{-1} of data, respectively. The photoproduction triggers for ZEUS required calorimetric energy to be deposited in the rear (photon) direction, and were of two types:

(a) "tagged"; requiring the detection of the scattered electron at very small angles, thereby limiting Q^2 to less than 0.02 GeV^2 and

(b) "untagged"; with no requirement on the detection of the scattered electron, but with energy deposition in the rear direction and the detection of at least one charged track. This allows the direct reconstruction of the photoproduced vector mesons decaying into charged track states. The offline requirement of the absence of a detected scattered electron in the main rear calorimeter limits Q^2 to less than 4 GeV^2.

The total "tagged" photoproduction cross sections $\sigma(\gamma p)_{\text{tot}}$ at HERA for the 1993 data [2, 3] are shown in Fig. 1, for $W_{\gamma p} \approx 200$ GeV. Also shown (solid circles) are lower energy measurements [4]. Global event characteristics are used by ZEUS to obtain the fraction of non-diffractive, inelastic diffractive, and elastic components to be 64.0%, 23.3%, and 12.7% respectively. Assuming that 82% of the elastic cross section is due to ρ^0 production

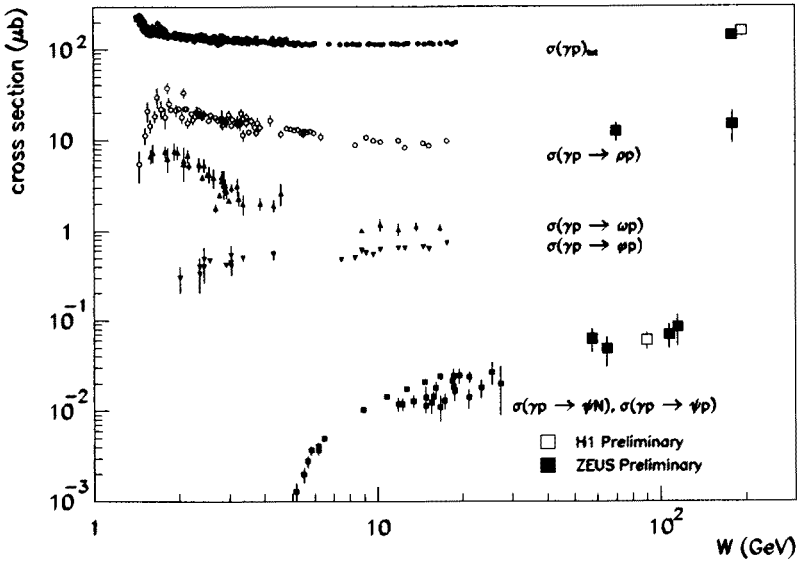

Fig. 1. Photoproduction cross section measurements from HERA and lower energy experiments.

yields an indirect measurement of the elastic cross section $\sigma(\gamma p \to \rho^0 p)$ to be 14.8 $\pm$5.7 μb, and this is shown in Fig. 1.

The direct measurement of the ρ^0 elastic cross section has been obtained by ZEUS from the "untagged" trigger at $60 < W_{\gamma p} < 80$ GeV. Two well reconstructed tracks of opposite charge coming from a good vertex are required, and an invariant mass is formed by assuming these two tracks to be pions. Events in which neutral particles are produced are rejected by requiring that there be less than 200 MeV in any calorimeter cell outside a limited region around the track direction.

Proton diffraction is a serious background, and in the absence of a fully equipped leading proton spectrometer, we require that there be less than 1 GeV in the forward calorimeter (*i.e.* the proton direction). Demanding $0.55 < m_{\pi\pi} < 1.0$ GeV reduces the contamination from other vector mesons. Finally, we limit the ρ^0 transverse momentum squared to be less than 0.5 $(\mathrm{GeV}/c)^2$ to further reduce the proton diffraction contamination.

The mass spectrum is shown in Fig. 2. The deviation from a Breit–Wigner shape for the ρ^0 is well known, and is caused by the interference (dashed-dotted) of the resonant $\pi^+\pi^-$ production (dotted) and a non-resonant background (dashed). A functional form of the three contributions is used to extract the resonant contribution to the cross section. The result is $\sigma(\gamma p \to \rho^0 p) = 12.5 \pm 0.7(stat) \pm 2.8(syst)$ μb, and is shown in Fig. 1, where lower energy data (open circles) are also shown for comparison [4].

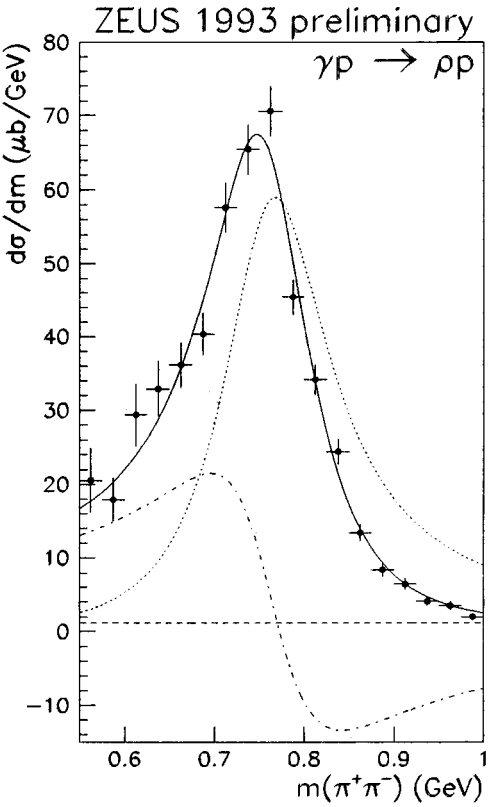

Fig. 2. Invariant mass distribution of $\pi^+\pi^-$.

ZEUS has performed a similar analysis to obtain a measurement of the elastic ϕ cross section for the decay channel ($\phi \to K^+K^-$). The invariant mass distribution is shown in Fig. 3. However, the cut on the ϕ transverse momentum squared is $0.2 < P_t^2 < 1.0$ $(\mathrm{GeV}/c)^2$, as the acceptance drops sharply below 0.2 $(\mathrm{GeV}/c)^2$ due to the geometry of the detector and the trigger. The average acceptance in the selected region is 20%. The elastic cross section $\sigma(\gamma p \to \phi p)$ within this restricted range in $W_{\gamma p}$ and P_t^2 is measured to be $278 \pm 30(\mathrm{stat}) \pm 78(\mathrm{syst})$ nb.

The investigation of the photoproduction of heavy quarks is a probe of strong interaction physics in a region characterised by the transition between perturbative QCD and non-perturbative interactions. The photoproduction of J/ψ is an ideal process to explore this regime. A clear signal can be seen from H1 in Fig. 4 from the invariant mass distribution of the sum of the electron and muon decay modes of J/ψ. The analysis for the measurement of $\sigma(\gamma p \to (J/\psi)p)$, where $J/\psi \to e^+e^-$ or $\mu^+\mu^-$, is covered elsewhere in

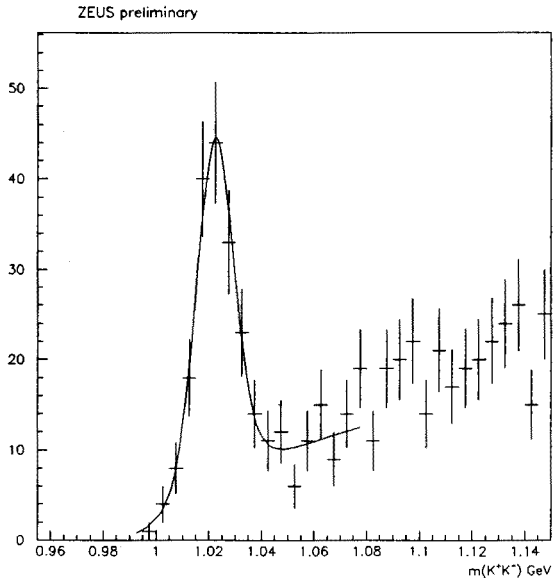

Fig. 3. Invariant mass distribution of K^+K^-.

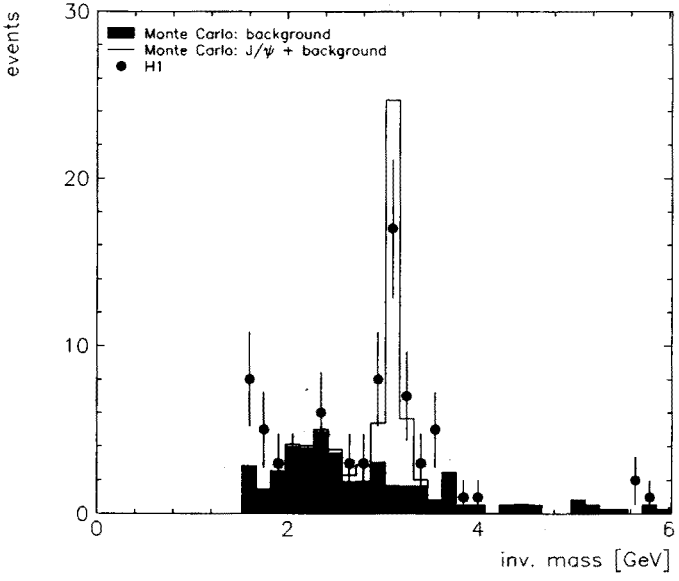

Fig. 4. Invariant mass distribution of e^+e^- and $\mu^+\mu^-$.

these proceedings, but the results are shown in Fig. 1 for H1 and ZEUS, along with lower energy data [4].

3. Inclusive transverse momentum distributions

Photon diffractive events are characterised by a gap in rapidity between the leading particle and the photon dissociated system of mass M_x, where the reaction is mediated by the exchange of a pomeron [5] having the quantum numbers of the vacuum. Detectors being installed in the very forward region will tag the recoiling proton for an unambiguous classification of diffractive events. The final implementation of these detectors is still in progress, and hence not used in this analysis.

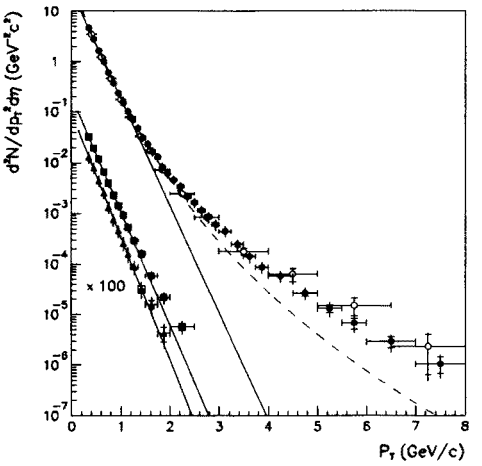

Fig. 5. Transverse momentum distribution of charged tracks for photoproduction events.

The tagged data sample has been divided into diffractive and non-diffractive subsets, according to the pseudorapidity[1] η_{max} of the most forward calorimeter deposit with energy above 400 MeV. We have found that a cut on $\eta_{max} < 2.0$ is very effective in separating the diffractive events from non-diffractive events.

The spectrum of transverse momenta P_t of tracks satisfying stringent quality criteria in diffractive events is shown in Fig. 5, where the data are displayed in two different M_x bins: triangles for $\langle M_X \rangle = 5$ GeV, squares for $\langle M_X \rangle = 10$ GeV. Here M_x is the relevant energy scale for the interaction.

[1] $\eta = -\log(\tan(\theta/2))$, where the polar angle is with respect to the proton direction.

Exponential fits (solid lines), normalised to the data points below 1.2 GeV/c, shows that the diffractive data points are consistent with such a fit.

The non-diffractive events are shown in the same figure for H1 (open circles, [6]) and ZEUS (solid circles). The dashed curve is a power law fit to UA1 [7] data for $p\bar{p}$ collisions at a centre of mass energy of 200 GeV. Although is not clear at what energies the comparison should be made, it is clear that the HERA data at similar energies have a harder spectrum. This is hardly surprising since, although the photon exhibits hadron-like properties, the parton distributions in the photon and proton are different, and also because the photon interacts directly.

4. Hard scattering in photoproduction

A deviation from the "soft" exponential term in Fig. 5 is an indication of hard interactions, and searching for jet structure is the next step, as jets are the observable objects most closely related to the partons. Both H1 and ZEUS have found jets in photoproduction events with transverse energy greater than 5 GeV. The partonic definition of x_γ in Eq. (1) is redefined to refer to the variables measured from the jets.

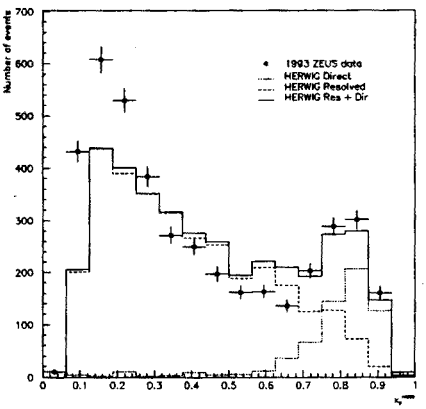

Fig. 6. x_γ distribution for data and HERWIG Monte Carlo with direct and resolved components.

Both ZEUS and H1 have evidence for the direct and resolved components in photoproduction through the variable x_γ, as seen from the distribution of x_γ from the ZEUS data in Fig. 6. Monte Carlo simulations are also shown for the resolved (dashed) and direct (dotted) contributions, and the sum (solid line). The operational definition used for the photon classification is that $x_\gamma < 0.75$ is "resolved" and $x_\gamma > 0.75$ is "direct".

At HERA, events with two observable jets ($E_T^{\rm jet} \gtrsim 6$ GeV, $\eta^{\rm jet} \lesssim 2$) are sensitive to x_p as low as 10^{-3} and x_γ of approximately 10^{-1}. We consider jets at nearly equal pseudorapidities, with an average of $\bar{\eta}$, as the configuration of "same-side" jets allows very small x values of the initial partons to be examined [8].

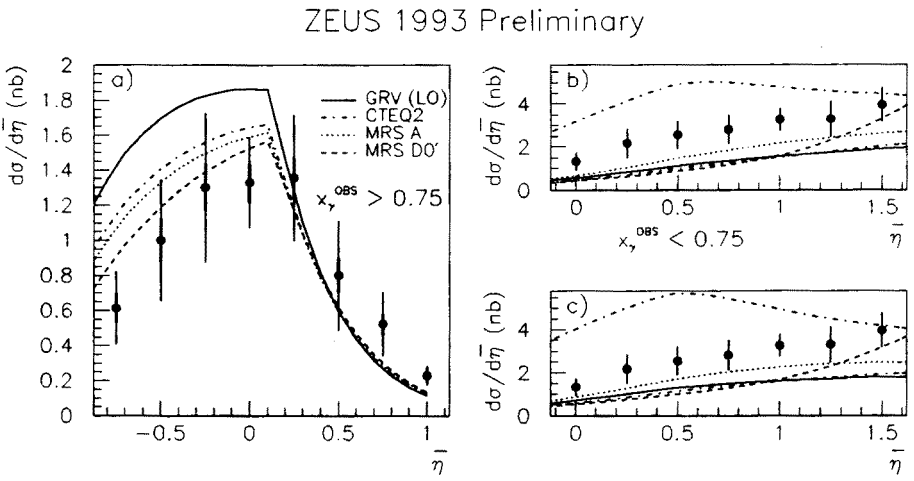

Fig. 7. $\bar{\eta}$ distribution for $x_\gamma > 0.75$ is shown in figure a). GS2 set was used for the photon, and the sets for the parton distribution for the proton were: GRV (solid line), CTEQ2 (dash-dotted line), MRSA (dotted line) and (MRSD0)' (dashed line). In figures b) and c), $x_\gamma < 0.75$ and the parton distributions for the photon are LAC3 (high, dash-dotted line), GS2 (dotted line), GRV (solid line), LAC1 (dashed line), and DG (low, dash-dotted line). The parton distribution for the proton was MRSA for figure b) and GRV (LO) for figure c).

The differential cross section in $\bar{\eta}$ for $x_\gamma > 0.75$ is dominated by direct photon interactions and so is insensitive to the parton distribution in the photon, but sensitive instead to the gluon distribution in the proton. This is shown in (Fig. 7a) (solid circles) and compared to LO QCD calculations using various parton distribution sets for the proton. Low-x effects such as non-zero k_T of the incoming partons may explain why the measured cross section lies below most curves at low $\bar{\eta}$ [9]. However, other higher order or hadronisation corrections have not yet been fully considered.

The region $x_\gamma < 0.75$ is sensitive to the gluon distribution in the photon. As the x_p values probed here are in the region where the parton densities of the proton are well constrained by other measurements, the sensitivity to different parton distribution sets in the proton is small as can be seen from a comparison of MRSA in Fig. 7b and GRV (LO) in Fig. 7c. However, the sensitivity to different photon parton distribution sets is large as can be

seen from the variations in the predictions. Higher order QCD calculations are necessary before strong conclusions can be drawn.

5. Hard diffraction in photoproduction

The observed properties of the diffractive cross section have been described by Regge theory, where the process proceeds through the exchange of the pomeron. The interplay of Regge theory and perturbative QCD is one motivation for studying hard scattering in diffractive processes [10], since these subjects are mostly without experimental overlap. In one such treatment of this subject [11], Ingelman and Schlein have modelled the pomeron as a hadron having constituent partons. The result of hard interactions is the production of jets, similar to the discussion in Section 4. Monte Carlo programs modelling a partonic interaction of the pomeron and based on pQCD now exist, (*e.g.* POMPYT [12]) and we can confront these with HERA diffractive data.

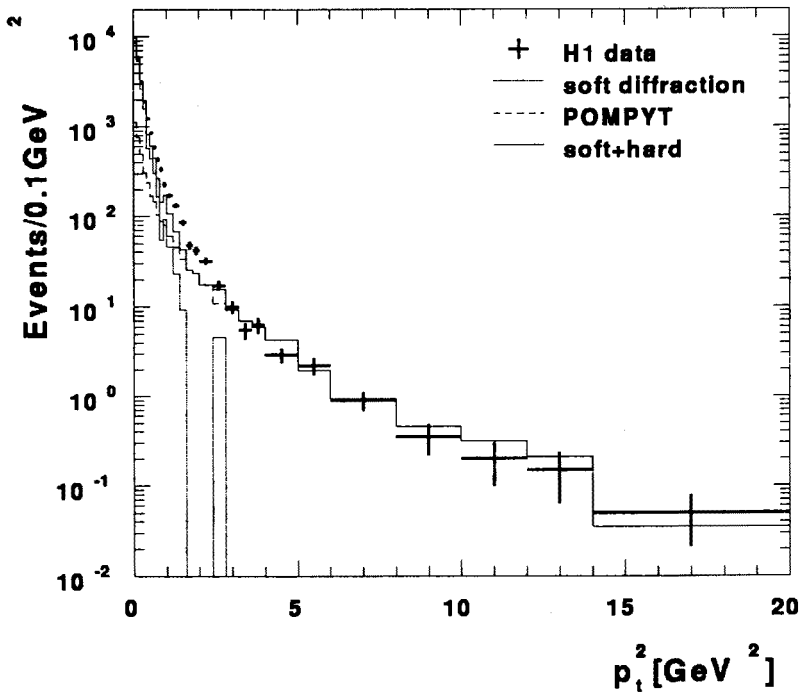

Fig. 8. Square of the transverse momentum distribution for photoproduction diffractive events from H1.

Fig. 8 shows the transverse momentum squared for diffractive events selected with $\eta_{\max} < 1.5$, from H1 data [13]. PYTHIA, which models

soft diffraction, cannot account for the high P_t^2 tail, but POMPYT, which models hard diffraction, reproduces this hard tail well, which could be an indication of hard partonic scattering in photon diffraction events.

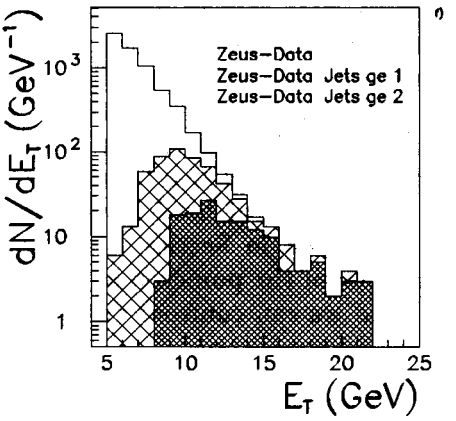

Fig. 9

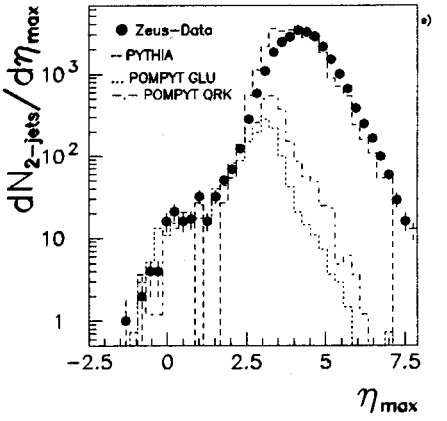

Fig. 10

Fig. 9. Transverse energy of diffractive events from ZEUS for all events with E_t greater than 5 GeV (solid line), and the subset with at least one jet (crossed), and greater than one jet (shaded).

Fig. 10. $\eta_{\max}$ for all γp events with two jets from ZEUS.

It is natural to search for jet structure in such diffractive events. Fig. 9 shows the transverse energy E_t spectrum for diffractive events with $E_t > 5$ GeV, and we see that 6.5% (2.1%) of the events have at least one (or more) jet(s). Jet production dominates the high E_t region, with jets having E_t as large as 10 GeV being observed.

To verify that this is not the tail of the non-diffractive data, we show in Fig. 10 the $\eta_{\max}$ distribution for photoproduction events with two jets in ZEUS. The excess of jets for $\eta_{\max}$ below 1.5 is not reproduced by photoproduction processes as modelled in PYTHIA, which predicts less than 0.1% of events with jets in this region, to be compared to the 0.63% seen. However, POMPYT, with hard interactions from a quarkonic (QRK) or gluonic (GLU) pomeron, gives a reasonable agreement in this region. These observations are consistent with hard partonic scattering in diffractive γp collisions.

The restriction on $\eta_{\max}$ imposes a limit in the range of phase space available for large masses and large E_t jets which are desirable for more conclusive studies of the hard interactions. We will cleanly identify diffractive events with the final implementation of the Leading Proton Spectrometers and the Forward Neutron Calorimeters in H1 and ZEUS. Already, ZEUS

has detected fully measured $\gamma p \to \rho^0 p$ events. High energy leading neutrons have also been observed for the first time. In addition to the diffractive processes, reactions from a pion exchange with the production of a forward neutron will also be investigated. The study of forward baryonic states will be an important aspect of the future physics programs at HERA.

6. Conclusions

We have reported on a wide range of physics results from photoproduction at HERA, from cross section measurements to detailed studies of the elastic and inelastic diffractive subprocesses. The large centre of mass energy of HERA has allowed the observation of the direct and resolved components of the photon interaction, and jets as evidence for hard scattering. We have found evidence of hard partonic scattering in diffractive γp collisions. With the final implementation of the forward detectors, we will be able to identify and explore the characteristics of high mass diffractive events.

We thank the DESY directorate for their strong support and encouragement. The remarkable achievements of the HERA machine group were essential and are appreciated. The author appreciates the time and effort invested by several H1 and ZEUS members during the preparation of this talk.

REFERENCES

[1] J.K. Storrow, *J. Phys.* **G19**, 1641 (1993).
[2] H1 Collaboration, *Phys. Lett.* **B299**, 374 (1993).
[3] ZEUS Collaboration, *Zeit. Phys.* **C63**, 391 (1994).
[4] A. Baldini *et. al., Landolt-Börnstein, Group I,* Vol 12b, ed. Schopper, Springer-Verlag.
[5] K. Goulianos, *Phys. Rep.* **101**, 169 (1983).
[6] H1 Collaboration, *Phys. Lett.* **B328**, 176 (1994).
[7] C. Albajar *et. al., Nucl. Phys.* **B335**, 261 (1990).
[8] J.R. Forshaw, R.G. Roberts, *Phys. Lett.* **B319**, 539 (1993).
[9] J.R. Forshaw, R.G. Roberts, *Phys. Lett.* **B335**, 494 (1994).
[10] E. Berger *et. al., Nucl. Phys.* **B286**, 704 (1987).
[11] G. Ingelman, P. Schlein, *Phys. Lett.* **B152**, 256 (1985).
[12] P. Bruni, G. Ingelman, DESY 93-187.
[13] S. Levonian, Proceedings on the Workshop on Two-Photon Physics at LEP and HERA, Lund, May 1994, p.96.